CARBON 47 (2009) 1693–1700

available at www.sciencedirect.com

ScienceDirect

journal homepage: www.elsevier.com/locate/carbon

Origin of friction in films of horizontally oriented carbon nanotubes sliding against diamond

Kausala Mylvaganam[a], *L.C. Zhang*[b,*], *K.Q. Xiao*[a]

[a]*School of Aerospace, Mechanical and Mechatronic Engineering, The University of Sydney, NSW 2006, Australia*
[b]*School of Mechanical and Manufacturing, The University of New South Wales, NSW 2052, Australia*

ARTICLE INFO

Article history:
Received 10 November 2008
Accepted 21 February 2009
Available online 3 March 2009

ABSTRACT

Carbon nanotube films were fabricated by a new deposition technique that can minimize carbon nanotube rolling/slipping when sliding against diamond. Molecular dynamics simulations were performed to understand the friction mechanisms. Results clarify the controversial arguments in the literature and conclude that the atomically smooth surface without dangling atoms and durability of the atomic lattice structure of carbon nanotubes makes them a good solid lubricant with an ultra-low coefficient of friction of around 0.01.

1. Introduction

Investigations into the tribological behaviour of carbon nanotube (CNT) reinforced composites have led to controversial outcomes. Nanotube based polymer, ceramic and metal composites have been considered to configure nano-structured surfaces and it was observed that the friction and wear properties were altered through the addition of nanotubes [1]. Some studies found that the addition of CNTs to a polymer matrix can reduce the friction coefficient and wear rate of the CNT-composite [1–4], but some others reported that the use of CNTs does not improve the composite's tribological performance [5,6]. This poses an interesting question: What are the true tribological properties of CNTs?

Measured friction coefficients of carbon nanotubes alone also vary widely [7–11] from 0.01 to 2.0. The coefficient of friction is not an inherent material property, but depends very much on the operating conditions and surface conditions. Several factors such as temperature, counter surface, atmospheric conditions and alignment of CNTs could affect the value of friction coefficient. For example, in vacuum, the measured friction coefficient of horizontally aligned multi-walled carbon nanotubes in contact with stainless steel fluctuated between 0.19 and 0.48, while in contact with alumina–yttria stabilized zirconia was between 0.07 and 0.11. In air, the coefficient of friction in contact with stainless steel was between 0.025 and 0.06 [9]. Studies on vertically-aligned CNT films [7,11] seem to have produced disappointing results, showing a very high coefficient of friction. Nevertheless, it was considered that these results do not really reflect the origin of the frictional behaviour of CNTs against their sliding counterparts because the bending and local buckling of the CNTs could have substantially influenced the force variation in the sliding direction in tests. A few studies examined the friction coefficient of transversely distributed CNT films manufactured by depositing CNTs in solvent onto a quartz disk. The measured friction coefficient on such CNT films varied from 0.04 [9] to 0.09 [11], almost an order of magnitude lower than that of the vertically-aligned CNT films. However, it was considered that the lower friction could be due to the rolling of CNTs during contact sliding similar to a suggested mechanism for the low friction of graphite [12,13], because the CNTs in the films made by the above deposition method were loosely stacked and they could roll or slip under lateral sliding forces. As a result, these measurements do not clarify the question about the origin of the frictional property of CNTs. Dickrell et al. [10] performed a series of tribological experiments on both films using a borosilicate glass counter surface at a normal load of 2 mN, sliding speed of 300 μm/s and a tract length of 600 μm, while varying the film temperature. They

* *Corresponding author:* Fax: +61 2 9663 1222.
E-mail address: Liangchi.zhang@unsw.edu.au (L.C. Zhang).
0008-6223/$ - see front matter
doi:10.1016/j.carbon.2009.02.020

found that the friction coefficient of the vertically-aligned film was approximately 10 times higher than the transversely distributed film and the friction coefficient monotonically decreased with the increase in temperature. They then considered that the friction coefficient of CNTs could be tuned by tailoring the contact temperature, thus providing a way of control of the friction coefficient. They explained the anisotropy of friction through the contact area variation with the CNT orientations. A few papers reported the tribological properties of CNT bundles based on theoretical investigations. For example, Ni and Sinnott [14] investigated the responses of bundles of single-walled CNTs to compressive and shear forces between two sliding diamond surfaces using classical molecular dynamics simulations. They obtained a friction coefficient of about 30 for sliding on horizontally arranged nanotubes at low load and 0.36 at a compressive pressure of 13.7 GPa. Because of these, they concluded that the conventional definition of friction coefficient is not appropriate for characterizing the tribological properties of CNTs.

This paper aims to understand the origin of the frictional behaviour of horizontally aligned CNTs under contact sliding against a diamond tip. To this end, we will investigate the problem in parallel in two ways. Experimentally, we will make thin films of densely packed, highly entangled CNTs and firmly bond them on solid glass substrates to allow high contact pressure friction test to proceed with minimized CNT rolling/slipping. Theoretically, we will carry out a series of molecular dynamics analyses in vacuum to understand the mechanism.

2. Experiment

Our manufacturing process of a CNT film as shown in Fig. 1 was as follows. First, a Loctite 460 glue was spread on to the top of a glass disk. A resin layer then formed after the solvent in the glue vaporized. This resin-on-glass substrate was placed in an oven at 70 °C for 2 h to enable the resin layer to harden. The top surface of the resin layer was then polished by diamond papers (9, 3 and 1 μm diamond abrasives, respectively) to make it ready for CNT bonding.

Meanwhile, multi-walled carbon nanotubes of about 15–30 nm in diameter and about 5 μm in length, prepared by chemical vapour deposition (provided by Nanolab), were ultrasonicated for 20 min in distilled water in a beaker. The resin-on-glass substrate was then placed in the beaker with the resin layer facing up to allow the dispersed CNTs to deposit onto the resin surface. The water was removed by heating at 70 °C in a vacuum oven. In this process, the carbon nanotubes penetrated into the softened resin layer at 70 °C which provided a strong bonding with the glass substrate after the solidification of the resin layer at room temperature. The CNT film made in this way can avoid or minimize the CNT rolling and slipping in friction experiments.

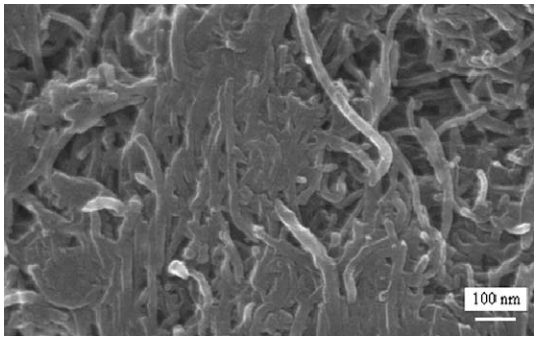

Fig. 1 – A CNT film that was developed with a resin, showing densely packed entangled CNTS.

The friction tests were performed on a micro-tribometer (made by CETR) under dry condition at room temperature. A conical diamond tip (tip radius ≈ 84 μm) was used to slide over the CNT film. Before testing, the diamond tip was cleaned with acetone in an ultrasonic bath. A sliding experiment was run at the track diameter of 12 mm with the CNT film disk rotating at the speed of 0.1 rpm. Three normal loads, 0.0098, 0.0294 and 0.049 N, were applied, respectively, on a stabilized sliding track formed under the normal load of 0.098 N. The friction coefficient was calculated from the ratio of the recorded tangential force to the applied normal load.

The morphologies of a CNT film before and after a friction test were examined using an FEGSEM6000 SEM at the voltage of 15 kV. SEM specimens were coated with a chromium thin film of 2 nm in thickness.

3. Theoretical investigation

For computational efficiency, in the molecular dynamics analysis, only single-walled carbon nanotubes (SWCNTs) were considered. Bundles consisting of (a) forty (17,0) zigzag SWCNTs of about 75 Å in length and (b) twenty (17,0) zigzag SWCNTs of about 150 Å in length were arranged horizontally in five rows in a closely packed arrangement as shown in Fig. 2a and b. CNTs on the bottom row were fixed and the other CNTs in the bundle were relaxed for 7500 time steps. Effects of different sliding directions were investigated as follows. For sliding along the transverse direction, i.e., 90° to the longitudinal axis of the SWCNTs, a hemisphere diamond tool of about 25 Å in radius was placed 3 Å above the centre of a CNT on the top row, first column as shown in Fig. 2a. The tool was moved in steps of 0.001 Å first vertically by 5 Å which corresponds to a penetration depth of 2 Å, and then laterally along the CNT stack as indicated in Fig. 2a. During sliding both the lateral forces and the normal forces were monitored. The lateral forces are denoted as positive when they act in the sliding direction. The sliding was also carried out under different penetration depths of the diamond tool, 7, 12, 14.5 and 17 Å.

In the sliding tests along the axial and at 45 degrees to the axial direction of the SWCNTs, as shown in Fig. 2b and c, the nanotube length used in the model was about 150 Å.

The inter-atomic interactions were described by a three-body Tersoff–Brenner potential [15,16] which allows the formation of chemical bonds with appropriate atomic rehybridization and has been used to simulate various deformation processes [14,17–20] of CNTs. The non-bonded interactions between the diamond tool and the CNTs were modeled with the Lennard-Jones potential [21]. As pointed out in our previous study [20], a proper use of thermostat scheme in the MD

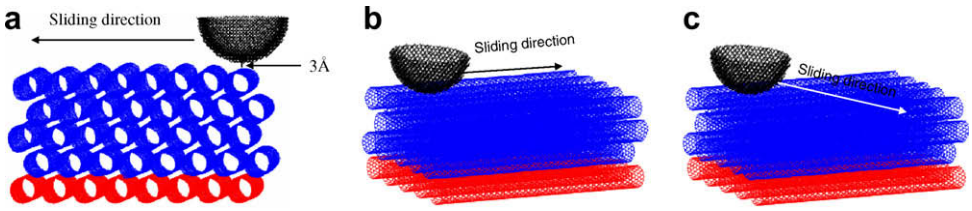

Fig. 2 – Initial model for sliding along (a) 90° to the longitudinal axis, (b) longitudinal axis, and (c) 45 degrees to longitudinal axis.

simulation of CNT is critical to producing meaningful results. Therefore in this work, we applied Berendsen thermostat on all the atoms (except the rigid ones).

4. Results and discussion

4.1. *Experimental observation*

Fig. 3 shows that using the new deposition method described above, CNTs penetrated into the resin layer to about 175 μm (Fig. 3a), and were wetted by the resin to form a CNT-resin composite zone (Fig. 3a–c). Hence, the CNTs were strongly bonded on to the substrate through the CNT-resin composite layer.

The morphology of the CNT film after a sliding test under a normal load of 0.098 N is shown in Fig. 4. On the film surface, we can see a clear sliding track, which is shining and can be even recognized by the naked eyes. The track surface is smooth and no CNTs were cut or broken. The average track width of the middle part is about 150 μm. Similar to other materials under scratching or indentation [22,23], there is a pile-up of CNTs at the track edge, indicating that the dense, networked CNTs in the film behave like a 'continuous material' under contact deformation.

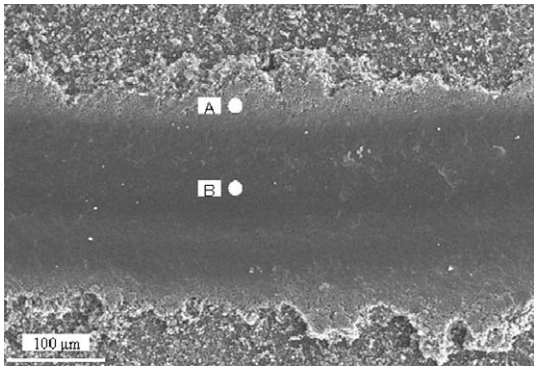

Fig. 4 – The friction track formed at a load of 0.098 N before formal testing. CNT film morphologies at the CNT pile-up area denoted as A and at the middle of the track as B were examined carefully and are shown in Fig. 5.

Fig. 5a and b demonstrates the surface morphologies of the CNT films at area A near the track edge, and that at area B near the middle of the track, respectively. These images reveal, compared with manufactured film (Fig. 1), that carbon nanotubes in the track were significantly compacted by the diamond tip during contact sliding. The nanotubes covered

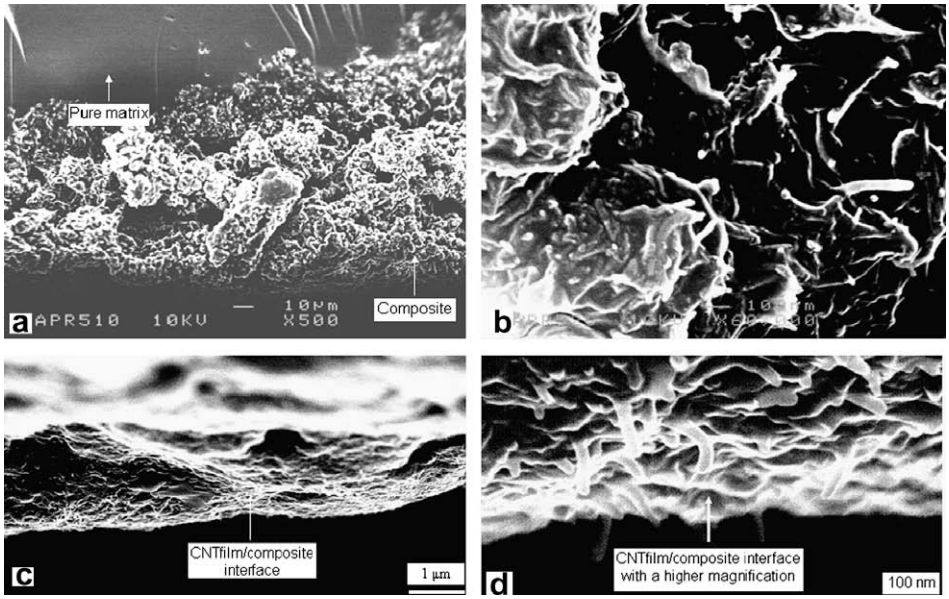

Fig. 3 – Cross section view of the composite, (a) the frontier of CNT penetration into the resin, (b) the formation of a composite, (c) CNT film/composite interface, and (d) the interface at a higher magnification.

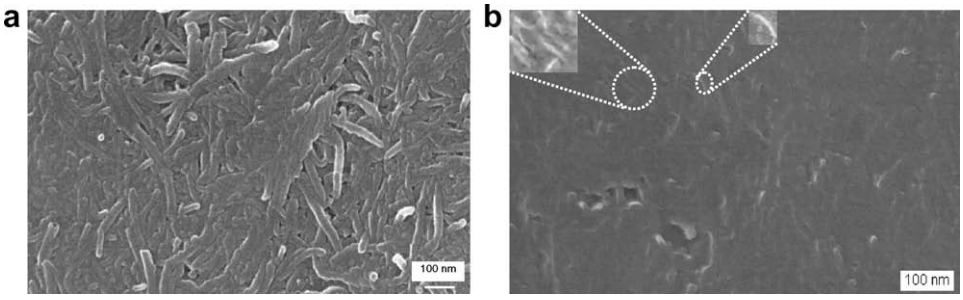

Fig. 5 – CNT images at the locations (a) A and (b) B (insertions show clearly the CNTs in the indicated regions), respectively, as shown in Fig 4, under the normal load of 0.098 N.

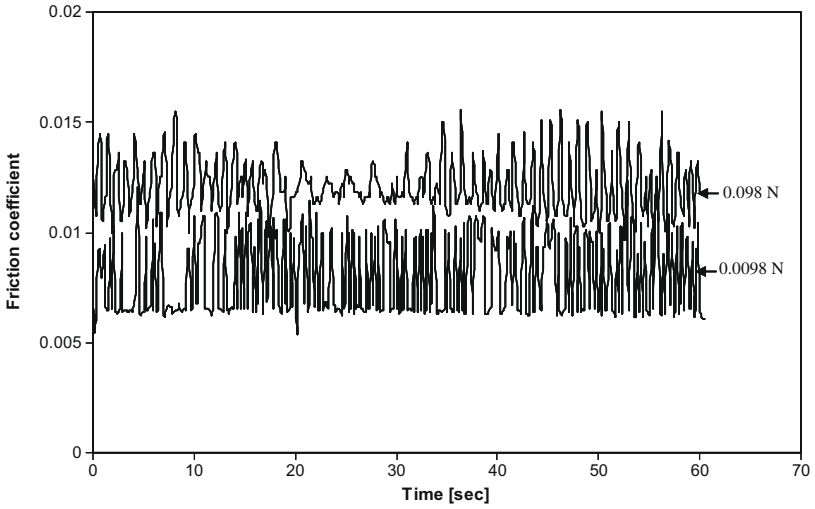

Fig. 6 – Friction coefficient of the CNT film at different normal loads. The tests were performed on the sliding track formed under the normal load of 0.098 N.

the whole track surface and even under the highest load in the present study, 0.098 N, they can be seen clearly in the image in Fig. 5b where insertions show more clearly the indicated regions, showing that the CNT film formed was stable during the friction test. It is evident that the film has a very high density of entangled CNTs so that when sliding on its top with the diamond tip, it was guaranteed that the friction measured was at the interface between the CNTs and diamond tip. Moreover, on the top of the film, the CNTs oriented mostly horizontally, but formed a complex network through their entanglements. Thus during a sliding test, the effect of rolling in using transversely distributed CNT films [9,11] and the influence of local buckling in using vertically-aligned CNT films [7–11] were reasonably eliminated.

Fig. 6 shows the friction coefficient variation with sliding time at the normal loads of 0.0098 and 0.098 N[1] .It can be seen that the friction coefficients vary slightly with different normal loads and has an average value of about 0.01. Compared with the 0.08 of high purity graphite tested at same condition, it is therefore reasonable to conclude that the CNT film is an excellent solid lubricant with an extremely low coefficient of friction, indicating that CNTs have tremendous potential of applications in the fields where ultra-low friction is required.

The whole area of the sliding track after formal testing has been observed carefully and the morphology of the CNTs is the same as shown in Fig. 5. The whole track is fully covered by carbon nanotubes. A careful examination of the nanotube morphologies does not show any trace of nanotube rolling, suggesting that the friction recorded in our experiment was due to the sliding at the interface between the CNT film and the diamond tip.

4.2. *Theoretical findings and understanding of low friction*

In the above experimental study, the nanotubes were entangled and oriented in all directions. Thus the sliding direction with respect to the nanotube longitudinal axis would vary from one CNT to the other. Therefore, we carried out the sliding simulations along three different directions, as shown in Fig. 2, to understand the different friction responses, if any, and hence to elucidate the experimental observations.

[1] The measured friction coefficients at the normal loads of 0.0294 and 0.049 N are very close to those in Fig. 6. For a better visualization, these friction coefficient curves are not included in Fig. 6.

4.2.1. *Sliding along 90° to the longitudinal axis*

On sliding under a low load of ~5 nN that is achieved by moving the tool down to 5 Å, as shown in Fig. 7a, the top row CNTs deform slightly and then recover as the tool moves away. However, by monitoring the atomic positions, we see that the top row CNTs spin by as much as 90° and the 2nd row nanotubes spin by about 50°, as shown clearly by Fig. 7c where an atom (labeled 1) in a first row nanotube moves circumferentially around the tube's axis by 90° but the axis of the nanotube does not show a noticeable lateral displacement during the diamond tip sliding. Hence the motion of the CNT represents a spinning.

On increasing the load to about 20 nN, by vertically moving the tool down to 15 Å, we can see that not only the CNTs on the top row but also those on the other rows deform significantly. Especially when the tool comes to a position in between two CNTs, the tubes in the second row deforms more as shown in Fig. 7b. In this case, however, the top row nanotubes spin around 60° and the 2nd row nanotubes spin less than 10°, because the CNTs are flattened more significantly and cannot spin as freely as in the previous low load case.

Throughout the sliding process, both the lateral and normal force fluctuated due to the changes in tool-CNT contacts as shown in Fig. 8a. This type of fluctuation of frictional and normal forces on the atomic scale is expected, of which the mechanism has been clearly explained by Zhang and Tanaka [24].

The conventional friction coefficient (the ratio of lateral force to normal force), μ, is shown in Fig. 8b. The average μ obtained by curve fitting varies between 0.03 and 0.06 for the different forces applied in this study, showing that it is not highly dependent on the loads at which the sliding is carried out.

4.2.2. *Sliding along the longitudinal axis*

In this sliding case, one atom on each end of a CNT was fixed to mimic the experimental situation where the length of the CNTs were much longer and could not move longitudinally. Depending on the position of the tool, the tool-CNT contact forces would vary. Therefore, in our simulation we have examined two different scenarios.

4.2.2.1. *(i) Tool positioned above the centre axis of a CNT.* On sliding under the low load of about 6 nN that is achieved by moving the tool down to 5 Å, a portion of the CNT below the tool flattened slightly. Other CNTs in the bundle did not show any noticeable deformation or rotation. When sliding under a higher load of about 28 nN, the CNT below the tool bent and flattened more obviously. In addition, all of its neighboring CNTs deformed to some extent but did not rotate. In both cases, the lateral force is very small compared to the normal force, giving a small friction coefficient of about 0.03. Fig. 9 shows the results when sliding under a load of about 6 nN. It is evident that here the friction coefficient is close to or lower than that when sliding takes place along the direction perpendicular to the longitudinal axis of CNTs as discussed in Section 4.2.1 above. This seems to indicate that the CNT spinning observed in Section 4.2.1 is not the cause of the low friction.

4.2.2.2. *(ii) Tool positioned above the gap of two CNTs.* In this set up, although the tip of the tool is in between two CNTs (i.e., directly above the gap), as the tool approach the CNTs it would be in contact with more CNT atoms and as

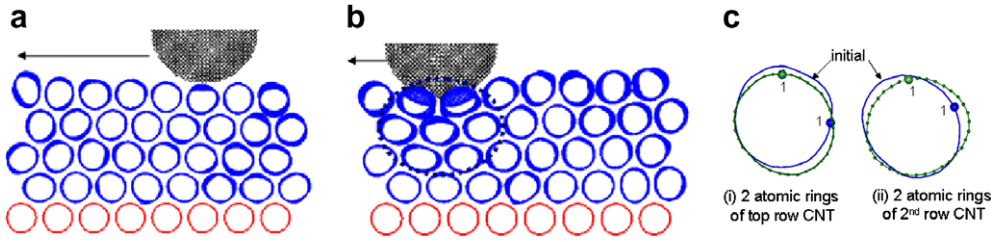

Fig. 7 – Deformation of CNTs on sliding (a) under 5.0 nN and (b) under 20.2 nN. (c) Illustration of CNT spinning under 5.0 nN; solid lines represents the initial position and ball and solid line represent the position after sliding.

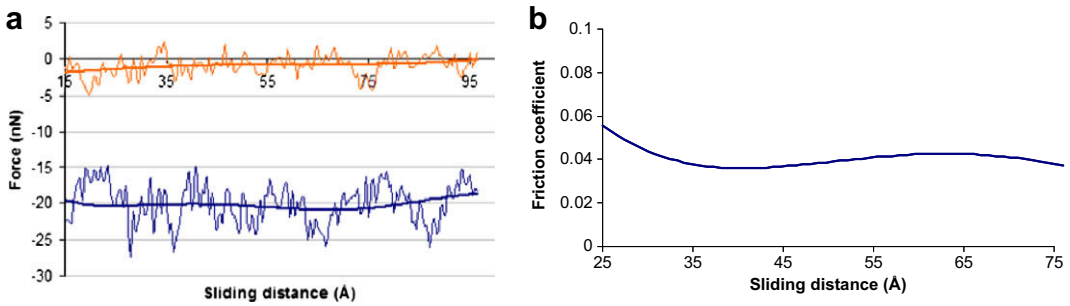

Fig. 8 – (a) Variation of lateral and normal force (b) average friction coefficient under a load of about 20.2 nN, during sliding in the direction 90° to longitudinal axis.

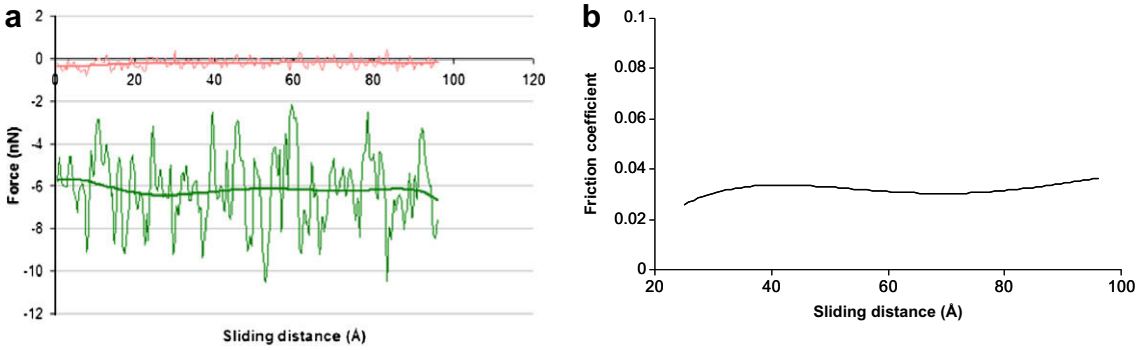

Fig. 9 – (a) Variation of lateral and normal force (b) average friction coefficient under a load of about 6.0 nN, during sliding along longitudinal axis.

such a higher force would be introduced. Moving the tool down vertically by 5 Å introduced a higher normal force of about 8 nN. Under this load, portions of the two CNTs on either side of the tool deformed and recovered as the tool moves away. Other CNTs in the bundle did not show any significant changes. When sliding under a higher load of about 26 nN, the neighboring CNTs on the top row as well as the CNT on the 2nd row directly beneath the tool got deformed significantly. Some CNTs on the 3rd row also deformed slightly as shown in Fig. 10.

Apart from the small variation in the deformation of CNTs and the magnitude of the forces, this setup of sliding led to an even lower friction coefficient, around 0.02 as shown in Fig. 10b. We see that the friction coefficient with the current sliding direction is lower than that when sliding takes place along the direction perpendicular to the longitudinal axis of CNTs as discussed in Section 4.2.1. This seems to show once again that the CNT spinning observed in Section 4.2.1 is not the cause of the low friction.

4.2.3. *Sliding at 45 degrees to the longitudinal axis of CNTs*

Under this sliding configuration, moving the tool down vertically by 5 and 15 Å introduces a normal force of around 7 and 28 nN, respectively. The average normal forces reached the steady value after the tool displaced about 30 and 40 Å, respectively. Because of the inclined direction, the tool would contact different CNTs during sliding, but we did not identify any noticeable spinning of the CNTs. The friction coefficient was found to be around 0.02, which is also lower than that when sliding along the direction perpendicular to the longitudinal axis of CNTs discussed in Section 4.2.1. Again, it seems that the CNT spinning previously observed is not the cause of the low friction.

4.3. *Discussion*

In all of our simulations, no CNT rolling occurred. The observed spinning of CNTs when sliding along 90° to the longitudinal axis does not seem to be the cause of low friction. To verify this, we repeated the sliding setup of Section 4.2.1 but fixed all the CNT ends to eliminate the CNT spinning. The result confirms that the average friction coefficient is still around 0.03.

Similar to our experimental findings presented in Section 3 which shows that the friction coefficient μ between CNTs and diamond is very low, around 0.01, our molecular dynamics simulations also show that μ is low varying from 0.02 to 0.06. The small discrepancy between the simulation and experimental results can be considered as the effect of sliding environment. The molecular dynamics simulations were conducted in vacuum while the experimental testing was done in open air, where the water vapour in the air between the tip and the nanotube could ease the friction. One may argue that in open air, due to surface passivation the adhesion and hence the frictional force can also reduce. However, nanotubes have a closed structure (i.e., no dangling bonds) with a large aspect ratio. Its surface passivation is negligible.

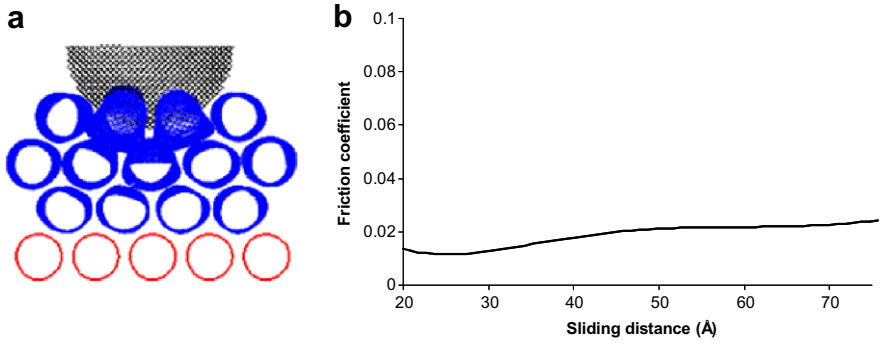

Fig. 10 – (a) Cross-sectional view of sliding along the axial direction under a load of about 26 nN with tool positioned in between CNTs (b) average friction coefficient variation under the same load.

Our investigations have clarified both experimentally and theoretically that unlike the friction mechanism of graphite [12,13], CNT spinning and rolling are not the origin of the low friction. We believe that the low friction phenomenon can be explained by the atomically smooth surface of a CNT as detailed below. A CNT is rolled from a graphite sheet. Hence, similar to a graphite sheet, a CNT is composed of planar sp2 hybridized carbon atoms, which gives an atomically smooth surface to the CNT. Because of the cylindrical shell structure of CNTs and their significantly large aspect ratio of length to diameter, horizontally oriented CNT films always maintain the same smoothness advantage across any length scale from nano to macroscopic dimensions. Hence, when a sliding is conducted on horizontally oriented CNTs, the friction can be extremely low regardless of the dimensional scale of the sliding test. One may argue that materials such as graphite and mica that has the smooth surface are known to have high friction coefficient in vacuum. Different materials have different specific characteristics. Although a graphite sheet has the same smoothness as a CNT, the surface of a bulk graphite at a larger scale (e.g., at the macro scale) always contain many atoms with dangling bonds because the graphite sheets of the bulk do not lay exactly in the plane of the sliding surface, due to either the surface roughness or the fabrication inability of a perfect alignment of the graphite sheets along the sliding plane. Thus on sliding in vacuum, diamond on graphite would give a higher adhesion force, and hence a higher friction coefficient, compared to diamond on carbon nanotubes without the dangling bonds. Assisting agents such as water vapour and oxygen in air can passivate a bulk graphite surface, leading to a low friction coefficient. This was verified by our experiment on graphite in air (Section 4.1), which showed that the friction coefficient between diamond and graphite in air is 0.08.

With mica, on the other hand, although it is also renowned in theory for its atomic smoothness, it is not so practically. A cleaved mica surface exhibits a hexagonal arrangement of Si (partly Al) and O atoms with partly covered potassium ions. The residual potassium ions react strongly with the constituents of the atmosphere yielding a carbon-containing contamination layer of 0.3–0.4 nm thickness. The absorbed contaminants on the surface do not get removed even on annealing under high vacuum conditions. With the aid of atomic force microscopy, Ostendorf et al. has shown that the surface has regularly shaped islands covered with a large number of small particles revealing a rough morphology [25]. Hence the high friction coefficient of mica could be due to its unsmooth surface.

A remaining question is: Will the hollowness of a CNT contribute to its property of low friction? To clarify this, we inserted a solid carbon nanowire passivated by hydrogen into each of the top row CNTs in the bundle and repeated the sliding simulations using molecular dynamics. The obtained friction coefficient is the same as before, i.e., from 0.02 to 0.06. This confirms that the hollowness of a CNT does not influence its frictional property, and that its atomically smooth surface without dangling atoms is the origin of its very low friction.

Finally, it is worth mentioning that in the sliding simulations, deformed CNTs upon sliding recover completely after sliding, indicating that the CNTs have a good durability. Thus the low friction coefficient together with their good durability make CNTs a good solid lubricant when the sliding is on the horizontally oriented surface of a CNT film.

5. Conclusions

This paper has identified the origin of low friction of horizontally oriented CNT films against the sliding of a diamond tip. It concludes that rolling, spinning or hollowness of a CNT does not contribute to the variation of the friction coefficient. The origin of its low friction is the CNT's atomically smooth surface without dangling atoms. Due to the cylindrical shell structure and the large aspect ratio of length to diameter of CNTs, the low friction property of CNT films can be maintained across any dimensional scales from nano to macro scales. This study has found that the friction coefficient of CNTs vs diamond in air is around 0.01. Hence, a horizontally oriented CNT film can be an excellent solid lubricant.

Acknowledgements

The authors thank the Australian research Council for its continuous financial support. This work was also supported by the Australian partnership for advanced computing.

REFERENCES

[1] Zhang LC, Zarudi I, Xiao KQ. Novel behaviour of friction and wear of epoxy composites reinforced by carbon nanotubes. Wear 2006;261:806–11.
[2] Zoo Y-S, An J-W, Lim D-P, Lim D-S. Effect of carbon nanotube addition on tribological behaviour of UHMWPE. Tribol Lett 2004;16:305–9.
[3] Dong JP, Tu JP, Zhang XP. An investigation of the sliding wear behavior of Cu-matrix composite reinforced by carbon nanotubes. Mater Sci Eng: A 2001;313:83–7.
[4] Chen WX, Tu JP, Wang LY, Gan HY, Xu ZD, Zhang XP. Tribological application of carbon nanotubes in a metal-based composite coating and composites. Carbon 2003;41:215–22.
[5] Satyanarayana N, Rajan KS, Sinha SK, Shen L. Carbon nanotube reinforced polyimide thin-film for high wear durability. Tribol Lett 2007;27:181–8.
[6] Liu LN, Gu AJ, Fang ZP, Tong LF, Xu ZB. The effects of the variations of carbon nanotubes on the micro-tribological behavior of carbon nanotubes/bismaleimide nanocomposite. Compos A: Appl Sci Manuf 2007;38:1957–64.
[7] Kinoshita H, Kume I, Tagawa M, Ohmae N. High frcition of a vertically aligned carbon-nanotube film in microtribology. Appl Phys Lett 2004;85:2780–1.
[8] Hu JJ, Jo SH, Ren ZF, Voevodin AA, Zabinski JS. Tribological behavior and graphitization of carbon nanotubes grown on 440C stainless steel. Tribol Lett 2005;19:119–25.
[9] Miyoshi K, Street Jr KW, Vander Wal RL, Andrews R, Sayir A. Solid lubrication by multiwalled carbon nanotubes in air and in vacuum. Tribol Lett 2005;19:191–201.
[10] Dickrell PL, Pal SK, Bourne GR, Muratore C, Voevodin AA, Ajayan PM, et al. Tunable friction behaviour of oriented carbon nanotube films. Tribol Lett 2006;24:85–90.
[11] Dickrell PL, Sinnott SB, Hahn DW, Raravikar NR, Schadler LS, Ajayan PM, et al. Frictional anisotropy of oriented carbon nanotube surfaces. Tribol Lett 2005;18:59–62.

[12] Bollmann W, Spreadborough J. Action of graphite as a lubricant. Nature 1960;186:29–30.
[13] Spreadborough J. The frictional behaviour of graphite. Wear 1962;5:18–30.
[14] Ni B, Sinnott SB. Tribological properties of carbon nanotube bundles predicted from atomistic simulations. Surf Sci 2001;487:87–96.
[15] Brenner DW. Empirical potential for hydrocarbons for use in simulating the chemical vapor deposition of diamond films. Phys Rev B 1990;42:9458–71.
[16] Brenner DW, Shenderova OA, Harrison J, Stuart SJ, Ni B, Sinnott SB. A second-generation reactive empirical bond order (REBO) potential energy expression for hydrocarbons. J Phys: Condens Matter 2002;14:783–802.
[17] Yakobson BI, Brabec CJ, Bernhole J. Nanomechanics of carbon tubes: instabilities beyond linear response. Phys Rev Lett 1996;76:2511–4.
[18] Mylvaganam K, Zhang LC. Nanotube bending due to central loading. J Comput Theor Nanosci 2005;2:251–5.
[19] Mylvaganam K, Zhang LC. Deformation-promoted reactivity of single-walled carbon nanotubes. Nanotechnology 2006;17:410–4.
[20] Mylvaganam K, Zhang LC. Important issues in a molecular dynamics simulation for characterizing the mechanical properties of carbon nanotubes. Carbon 2004;42:2025–32.
[21] Allen MP, Tildesley DJ. Computer simulation of liquids. Oxford: Clarendon Press; 1987. p. 21.
[22] Zarudi I, Zhang LC, Swain MV. Behavior of monocrystalline silicon under cyclic microindentations with a spherical indenter. Appl Phys Lett 2003;82:1027.
[23] Zarudi I, Zhang LC. Structure changes in mono-crystalline silicon subjected to indentation – experimental findings. Tribol Int 1999;32:701–12.
[24] Zhang LC, Tanaka H. Towards a deeper understanding of wear and friction on the atomic scale – a molecular dynamics analysis. Wear 1997;211:44–53.
[25] Ostendorf F, Schmitz C, Hirth S, Kühnle A, Kolodziej JJ, Reichling M. How flat is an air-cleaved mics surface. Nanotechnology 2008;19:305705.